PAPER

Check for updates

Preparation of ashless cellulose paper standards for rapid determination of multi-element concentrations in airborne fine particulate matter using laser ablation inductively coupled plasma mass spectrometry†

Lei Qiao, [ID] bc Ruijie Zhang,a Jing Qiao,a Xiaoyan He [ID] *a and Zhiwei Wuc

In this study, we developed ashless cellulose filter papers as calibration standards in laser ablation inductively coupled plasma mass spectrometry (LA-ICP-MS) to rapidly determine multi-element concentrations in airborne fine particulate matter ($PM_{2.5}$). To achieve this, the papers were treated by immersion in standard solutions, followed by evaporation of the solutions. The homogeneity of the paper standards was studied, and the results demonstrated that the elements were homogeneously distributed at the paper centers with slight fluctuations (*i.e.*, relative standard derivation $\leqq$ 8%). The instrument signal drift and instability were compensated using a pseudo internal standard (^{197}Au). The limits of detection established for LA-ICP-MS were obtained by the ablation of 11 lines on the procedural blank filter paper containing 0.5% HNO_3, with values ranging from 0.01 (Sr) to 0.49 µg g^{-1} (Fe). The accuracy of the LA-ICP-MS determinations was validated using certified reference materials (CRMs) and analyzed using six line scans. The results showed acceptable analytical errors (<13%). Thus, our method was applied to analyze actual $PM_{2.5}$ samples. Moreover, the sources of $PM_{2.5}$ in Hangzhou were also investigated. Additionally, this method has considerable potential for multi-element analysis in other airborne dusts.

1. Introduction

Recently, severe haze events have frequently occurred in large areas of China and have aroused widespread public concern. Fine particulate matter with an aerodynamic diameter of 2.5 µm or less is categorized as $PM_{2.5}$, especially the particulate matter emitted as a result of anthropogenic activities (*e.g.*, emissions from vehicle exhaust, coal burning, and industrial activity), and such matter is closely related to haze. These particles penetrate the respiratory system and seriously affect human health, causing serious economic and health burdens.[1–3] Because $PM_{2.5}$ may contain a variety of trace and toxic elements and penetrate the human lungs or blood vessels, heavy element concentrations (HEC) in $PM_{2.5}$ have been extensively studied in the past.[4–6]

Common crustal elements such as Mg and Fe in $PM_{2.5}$ mainly come from sand or building dust, which are dangerous and lead to haze and visibility reduction. Many toxic metals such as Cu, Zn, Cr, Cd, and Pb are trace elements in $PM_{2.5}$, which may accumulate in the human body and cause permanent damage.[7–9] Various techniques such as atomic fluorescence,[10] inductively coupled plasma spectroscopy/mass spectrometry[11] and atomic absorption[12] have been routinely employed to determine HEC in $PM_{2.5}$. Prior to analyses using these methods, $PM_{2.5}$ samples are usually prepared as solutions via dissolution steps such as chemical attack using an oxidizing (HNO_3) or a hazardous (HF) acid under high temperature conditions. Although these processes have been well established and satisfy most requirements, the digestion procedure is usually complicated and tedious as it consumes more acid and time than a direct sampling method, substantially limiting the analysis throughput. Additionally, it can cause the loss of volatile components during digestion or increase the spectral overlap of polyatomic peaks (*e.g.*, $^{40}Ar^{35}Cl^+$ on $^{75}As^+$).[13] Therefore, direct $PM_{2.5}$ analysis without complex sample preparation has long been a topic of great interest.

In view of the characteristics of HEC in $PM_{2.5}$, the combined use of the LA and ICP-MS systems is a perfect choice because this technology combines sample collection, transmission, atomization, and ionization in one step and has good sensitivity and a low detection limit. Furthermore, because no solvent is

aSchool of Life Sciences, Anhui Medical University, Hefei 230032, China. E-mail: hexiaoyan@ahmu.edu.cn

bSchool of Basic Medical Sciences, Anhui Medical University, Hefei 230032, China

cFocused Photonics Inc, Hangzhou 310000, China

involved in the sample transfer process, not only is the transfer efficiency high, but the interference of polyatomic ions caused by common reagents is also avoided, and this has attracted the attention of several analysts.[14–16] However, until now, the HEC in $PM_{2.5}$ has rarely been determined by LA-ICP-MS because of the lack of commercial or appropriate calibration standards. These standards need to overcome the problems of nonstoichiometric ablation, aerosol transport, atomization, ionization, and instrument signal drift during the analysis of $PM_{2.5}$ using LA-ICP-MS, which are still the main defects that hinder the accuracy and precision of this technology.[17–19]

In recent years, multiple quantitative analysis methods have been reported, including external calibration with or without internal standardization, solution-based calibration, and isotope dilution.[20–23] In general, external calibration strategy using solid certified materials (CRMs) that match the composition of an actual sample is the most reliable quantitative analysis method for LA-ICP-MS. There are several commercial solid CRMs for different types of materials such as glass and ceramics; unfortunately, they cannot cover every type of sample (*e.g.*, biological tissues or mineral compositions). As mentioned above, for each given element, the composition of the matrix may affect signal intensity differently during LA-ICP-MS analysis. Therefore, these solid CRMs are not suitable for the quantitative analysis of the information regarding elements on a filter membrane. Research on the synthesis of LA-ICP-MS calibration standards is being conducted extensively, including the preparation of self-made matrix-matched laboratory standards using the pelletization technology and adding known amounts of elements into similar matrix materials for biological or geological samples.[24–26] For example, to image trace metal distribution in tissue sections using LA-ICP-MS, Lear *et al.* prepared thick sections of matrix-matched tissue standards from chicken breast tissue spiked with standard solutions, which were then frozen, sectioned, and placed onto glass microscope slides for analysis.[27,28] Additionally, Ugarte *et al.*[29] synthesized homogeneous hydroxyapatite standard *via* the co-precipitation of calcium nitrate tetrahydrate and ammonium dihydrogen phosphate before the precipitate pressed into pellet. Unfortunately, when LA-ICP-MS is used to quantitatively analyze metals in environmental particles, it is difficult to prepare homogeneous air particulate standards using pelletization technology or by adding known amounts of elements to polytetrafluoroethylene or quartz filters. Thus, other strategies to prepare matrix-matched calibration standards for quantitative analysis of HEC in environmental particles have also been attempted, for example, Wang *et al.*[30,31] analyzed the concentrations of Cr and Si in airborne particulates by preparing simulated membrane-filter standards from National Institute of Standards and Technology (NIST) 1648a (urban aerosol). However, they proposed that the designed sampling chamber is complex and the preparation process is time-consuming. Furthermore, Tang *et al.*[18] quantitatively analyzed metals in environmental particles by evaporating and drying standard solution droplets on the surface of a quartz filter to prepare approximate matrix-matched external standards for LA-ICP-MS analysis. However, the prepared standards lacked sufficient homogeneity and reproducibility. A completely new approach was demonstrated by Nunes *et al.*[32,33] who successfully used ashless cellulose paper as a dropping solution support for plant analysis. This method is simple in terms of operation, easy to handle, and uses a wide calibration range (up to 250 µg g^{-1}), which brings great promise with regard to the preparation of a self-made standard for the LA-ICP-MS analysis of $PM_{2.5}$ samples. Nevertheless, the cellulose paper has not yet been further used as a calibration standard to evaluate HEC in airborne particulate matter using LA-ICP-MS.

To compensate for the matrix-related effects (difference of material ablation, aerosol transport, and analyte ionization) and instrument-related effects (signal drift and instability), internal standards (ISs) are usually combined with matrix-matched external standards to improve the reliability of qualitative analysis. As for the ashless paper used as the external calibration standard of LA-ICP-MS, carbon may be used as an IS because of its abundant and relatively homogeneous in ashless cellulose filter paper. However, the content of organic carbon and elemental carbon in the actual $PM_{2.5}$ samples may be different from that in the self-made standard sample. Previous studies have reported that as a feasible alternative strategy, Au, which is usually not present or is present in a very small amount in actual samples, can be artificially sputtered as a pseudo internal standard element to improve the precision and accuracy of LA-ICP-MS.[33,34]

In summary, this study aimed to use precut ashless cellulose filter papers that have been immersed in reference solutions and combined with a thin gold layer to develop a novel calibration strategy for LA-ICP-MS rapid analysis of HEC in $PM_{2.5}$. Furthermore, the homogeneity of the self-made paper standards and the parameters of laser ablation were studied. Finally, the established calibration strategy was applied to determine the HEC in actual $PM_{2.5}$ samples in Hangzhou. Moreover, we used the mass concentrations of $PM_{2.5}$ particles to investigate local seasonal variations and the enrichment factor (EF) model to study $PM_{2.5}$ sources.

2. Material and methods

2.1. Reagents and samples

High-purity water (resistivity: 18.2 MΩ cm) was obtained from ELGA (Purelab flex 2, UK) for material cleaning and solution preparation. Standard reference solutions (1000 µg mL^{-1}) of single elements were purchased from Agilent Technologies (USA); Pluronic F-127 (Sigma-Aldrich, USA) was used as the nonionic surfactant in the calibration solutions. Ashless cellulose filter paper (cellulose filter, no. 41) was obtained from Whatman, Clifton, NJ. Certified reference materials NIST 1648a (urban dust), 1573a (tomato leaves), and 610 (silicate glass) were obtained from the National Institute of Standards and Technology.

2.2. Instrumentation

Laser ablation was carried out using an Analyte HE 193 nm ArF Laser Ablation system (Photon Machines, USA) equipped with

a SQUID signal smoothing device for the *in situ* analysis of $PM_{2.5}$ samples, which was coupled with an Agilent 7900 ICP-MS (Agilent Technologies, USA). In LA-ICP-MS, the ablated aerosol in the cell was transported to the ICP-MS system by helium (He) through a 1.0 m polyethylene tube. Prior to every experiment, the LA-ICP-MS were preheated 30 min before operation and optimization. NIST silicate glass reference material of the NIST 610 was employed for optimizing the coupling before the analysis, for the maximum intensity of the $^{139}La^+$ signal and minimum formation of oxide (representing $^{232}Th^{16}O^+/^{232}Th^+ < 0.5\%$), and to keep the U^+/Th^+ ratio close to 1, and the tuning methods employed have been previously described by Yuan *et al.*[35,36] The optimized instrument operating parameters are summarized in Table 1. The background and analyte signals off-line selection, integration, and quantitative calibration were performed using an in-house software, LAICPMSDataCal.[37]

2.3. Preparation of paper standards

To reduce the interference of background elements in the filter paper, it was soaked in 5% (v/v) nitric acid and stirred overnight, followed by drying at 30 °C in a super-clean room. The paper was then carefully cut into approximately 8.0 mm diameter sizes using a steel punching tool and weighed in a microbalance with a resolution of 0.002 mg (26-1x, Secura®, Sartorius, Germany), with the aid of ceramic tweezers. The concentrations of the stock reference solutions (Mg, K, Cr, Mn, Fe, Ni, Cu, Zn, As, Sr, Cd, Ba, and Pb) ranged from 0 to 500 mg L^{-1}, which were prepared using "0.5% HNO_3 + 0.1% nonionic surfactant Pluronic F-127".[38] The concentrations were chosen as calibration standards for the range of interest analytes in typical $PM_{2.5}$ samples. The paper was immersed in the solutions, stirred for 48 h, and then quickly dried at 80 °C for 120 s in an infrared apparatus (Spectral Systems, Germany). The outer edge of the filter (approximately 2 mm) was cut off and attached to the glass slides with a double-sided adhesive tape, and the background signals of the related elements of the glass slide and tape were subsequently tested. Filter immersed in 0.5% HNO_3 was used as the blank sample. In addition, before LA-ICP-MS measurement, the self-made paper was covered with a thin layer of gold as a pseudo IS. The layer was sputtered using a B7340 instrument

(Agar Scientific Limited, Essex, UK) and carried out at a pressure of 0.1 mbar for 6 s. Twenty replicates of the paper standard preparation for each concentration level to obtain statistical significance of the data were carried out.

Further, the effective concentrations of the absorbed elements in the self-made paper standards were determined using the pneumatic nebulization ICP-MS (PN-ICP-MS) technology. The solution introduction system consisted of a cooling swirling fog spray chamber, Teflon concentric nebulizer, and torch. Parameters such as gas flow rate, torch position, lens voltages, quadrupole settings, and electron multiplier settings were optimized by tuning.

2.4. Collection of $PM_{2.5}$ samples

From January 2019 to February 2020, actual samples were collected at two sampling points, Bin'jiang (BG) and Lin'an (LN), (Fig. S1†) in Hangzhou every Saturday with an 8 h sampling period using a gas sampler PMS-200M (Four-channel Sampler, Focused Photonics Inc., Hangzhou, China) with a nominal flow rate of 0.5 m^3 h^{-1}. A total of 240 $PM_{2.5}$ samples were collected on ashless cellulose filters at each point. The distance between the two points was approximately 35 km. BG (30°18′N, 120°19′E) was classified as an urban sampling point, with a gas sampler located on the roof of a building in Focused Photonics Inc., approximately 15 m above the ground, and it is only 20 m away from the heavy traffic of Binan Road located to its south. LN (30°25′N, 119°83′E) is a hilly area in the suburbs, beside the Qingshan Lake, and is surrounded by farmland. Sampling at this point was carried out on the roof of a building of Puyu Technology Inc. Co. Ltd., approximately 10 m above ground level. Relevant meteorological data such as average temperature, average wind speed, and average relative humidity were recorded during the sampling period. These values were in accordance with the climatic parameters of Hangzhou collected from Weather Underground (http://www.wunderground.com/). After determining mass concentration, each sample was cut into a 6 mm diameter disk from the center for LA-ICP-MS analysis.

2.5. Preparation of ablation samples

A quartz glass disk (40 mm radius and 5 mm thickness) adhered with a double-sided tape was used to support the paper standards and actual samples. As shown in Fig. 1, the sample was operated by ceramic tweezers (each diameter was 6 mm). After all the samples and standards were loaded, the glass disk was coated with a thin gold layer. In this study, more than 20 samples and standards could be loaded on the developed glass disk in a 21 cm^3 ablation cell for subsequent analysis, avoiding the instability of the ICP-MS system during the step of frequently changing the sample in the ablation cell. The powder material of NIST 1648a was digested with strong acid, diluted with 0.5% HNO_3 + 0.1% Pluronic F-127 to an appropriate concentration, and then adsorbed by cellulose paper prior to LA-ICP-MS analysis. A pellet presser was used to make NIST 1573a pellets. Pressed powder disks with good mechanical stability could be obtained at a pressure of 30 MPa for 10 min (YP-40T, Tianjin) without the addition of a binder.

Table 1 Operating parameters for PN-ICP-MS and LA-ICP-MS analyses

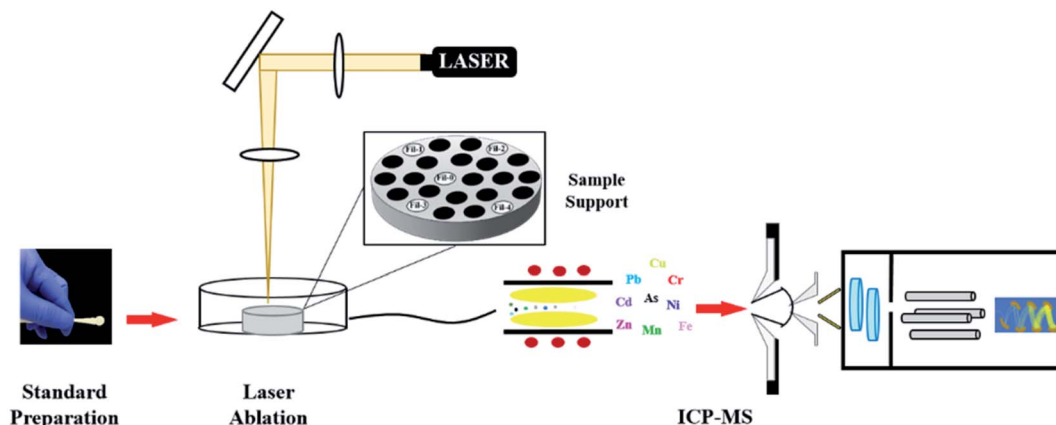| Parameter	PN-ICP-MS	LA-ICP-MS
RF power	1550	1500
Plasma Ar flow rate, L min^{-1}	15.0	15.0
Auxiliary Ar flow rate, L min^{-1}	1.00	1.00
Nebulizer Ar flow rate, L min^{-1}	0.90	—
Dwell time, ms	30	5
Carrier He flow rate, L min^{-1}		0.6
Energy density, J cm^{-2}		8
Repetition rate, Hz		10
Monitored isotopes, m/z		^{24}Mg, ^{39}K, ^{53}Cr, ^{54}Fe, ^{55}Mn, ^{60}Ni, ^{63}Cu, ^{66}Zn, ^{75}As, ^{88}Sr, ^{111}Cd, ^{137}Ba, ^{197}Au, ^{208}Pb

Fig. 1 Schematic diagram of the self-made paper standards and samples attached to glass disk support for LA-ICP-MS analysis.

3. Results and discussion

3.1. Mass analysis

Because temperature and humidity obviously influence the mass of filter paper, all papers were equilibrated at a constant temperature of $20 \pm 1\,^{\circ}\text{C}$ and relative humidity of $40 \pm 5\%$ for 24 h before and after sampling, and weighed three times. If the three values differ by $>10\ \mu\text{g}$, the three measurements are considered invalid and are repeated. After weighing, the filter papers were sealed and stored in a refrigerator at about $-20\ ^{\circ}\text{C}$ away from light prior to quantitative analysis to prevent the introduction of contaminants and evaporation of volatilized components.

At BG and LN, the annual mean concentrations of $PM_{2.5}$ were 63 and $52\ \mu\text{g m}^{-3}$, respectively, which exceeded the annual limit of $35\ \mu\text{g m}^{-3}$ for ambient $PM_{2.5}$ released by NAAQS-China. Significant seasonal variations in mean mass concentrations for heavy metals in $PM_{2.5}$ were observed at these two sampling points (Fig. 2). At BG, the maximum mean concentrations of

$PM_{2.5}$ appeared in winter ($74\ \mu\text{g m}^{-3}$) and the minimum in summer ($33\ \mu\text{g m}^{-3}$), while at LN, they decreased in the order of winter ($61\ \mu\text{g m}^{-3}$) > spring ($56\ \mu\text{g m}^{-3}$) > autumn ($48\ \mu\text{g m}^{-3}$) > summer ($29\ \mu\text{g m}^{-3}$). The two sampling points have similar seasonal variations, which may be attributed to local climatic conditions. In winter, the airflow in Hangzhou is stable, rainfall is less, and temperature is low, which are unfavorable for the diffusion or dilution of particulate matter. These variations might also be due to the increase in local anthropogenic pollution emissions, such as from vehicles, industries, firework displays, *etc.* In summer, Hangzhou often experiences precipitation and gale, which can efficiently remove and reduce atmospheric particulate matter. Therefore, to some extent, the mass concentrations of $PM_{2.5}$ could reflect local climate characteristics.

As described for the dried standards, the actual samples were covered with a thin gold layer after mass analysis. The specimens were divided into two parts, half of which were used for PN-ICP-MS to determine the reference concentration, and
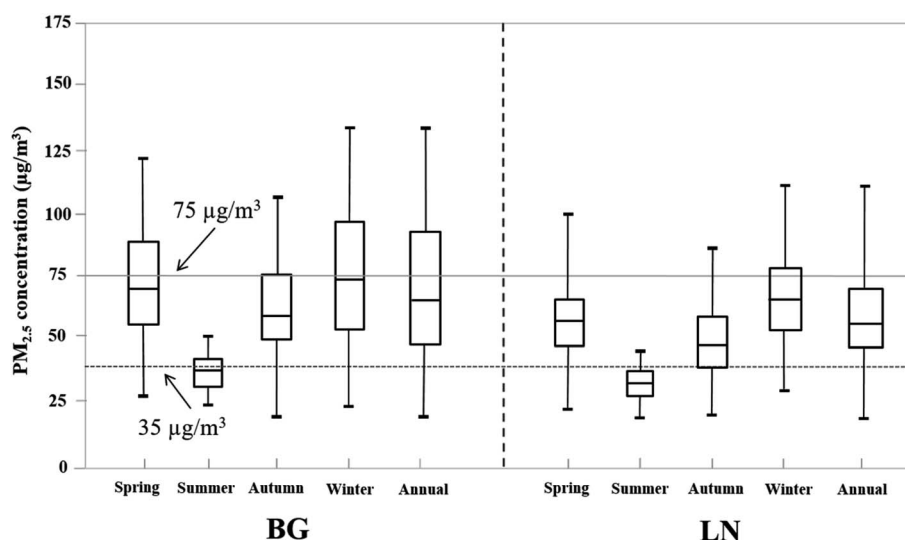

Fig. 2 $PM_{2.5}$ seasonal concentrations at BG and LN.

the other part was wrapped in annealed aluminum foil and stored in clean polyethylene bottles at <-20 °C until LA-ICP-MS analysis.

3.2. Elements analysis using LA-ICP-MS

3.2.1. Ablation parameters. Because laser energy directly affects ablation depth, the element concentrations in the self-made paper standards, double-sided tape, and glass slide are different. To prevent the difference in laser ablation depth from affecting the analysis signal and avoid contamination from the glass slide, the ablation parameters of LA-ICP-MS were carefully considered. Under the operating conditions for LA-ICP-MS analysis (Table 1), the glass slide (G), double-sided tape + glass slide (D-G), blank filter paper + double-sided tape + glass slide (B-D-G), self-made paper standards + double-sided tape + glass slide (S-D-G), and actual $PM_{2.5}$ samples + double-sided tape + Glass slide (A-D-G) were all ablated using four sequences by the laser at the same position, each for two seconds. As shown in Fig. 3a, the glass slide homogenously contains a little more ^{208}Pb than that of the blank filter disk. Furthermore, the signal intensities of ^{208}Pb obtained from the second sequence on the B/S/A-D-G was at the same level as for the first ablation time of B-D-G. Similarly, the determined signals for the second sequence of the laser on the D-G were at the same level as for the first sequence of G. Other elements showed similar behaviors, and these results demonstrated that under the optimized laser energy parameters (Table 1), contamination from the double-sided tape or glass slide could not be introduced.

3.2.2. Homogeneous of self-made filter paper standards. The homogeneity of the analyte distribution in the filter paper standards was of utmost importance for reliable LA-ICP-MS calibration and was evaluated by ablating three spatially random ablation lines across the entire paper disk (approximately 7.6 mm), with an ablation diameter of 60 μm and a scan speed of 30 μm s^{-1}. The raw intensities of ^{208}Pb and one of the

intensities of the pseudo internal standard of ^{197}Au were illustrated by ablating the paper immersed in aliquots of 50 mg L^{-1} standard solution (Fig. 3b). We observed that the analyte absorbed in the solid paper disk was almost homogeneous, although the elemental concentration at the center is slightly lower than those of the edges of the filter. Furthermore, the results shown that elements were homogeneously distributed in the ashless cellulose paper centers with slight fluctuations (RSDs $\leqq$ 8%), which meets the crucial requirement for an LA-ICP-MS reference material. In addition, the signal intensity distribution was symmetric to the center of the filter paper, and other elements of interest absorbed in the standard showed similar results. These phenomena may be due to chromatographic effects during drying or the edge effect of the paper, which was looser than the center and easier to be ablated by LA.[18] Therefore, in this study, the paper outside was symmetrically cut out (approximately 2 mm), that is, 6 mm of the paper piece (the dotted circle in Fig. 3b) was retained for LA-ICP-MS analysis. Furthermore, the signal intensity of Pb obtained from the third ablation line at the point of ablation intersection was equivalent to those of the other two lines, further confirming that the contamination from the double-sided tape + glass slide (D-G) could be avoided from the optimized LA parameters. In addition, because the ablation spot of LA was <200 μm and deposition of atmospheric particles on the surface of the filter was inhomogeneous, for direct sampling of solid $PM_{2.5}$ samples by LA-ICP-MS, six lines were parallelly ablated along the filter diameter direction using line scan mode. The average value of the element signal intensity was taken into consideration for data processing.

3.2.3. LA-ICP-MS calibration using paper standards. The effective concentrations of the adsorbed elements in the self-made paper standards were determined using PN-ICP-MS to generate calibration curves, followed by digestion with a microwave digestion system (WX-8000, PreeKem, China). The samples and blank papers were attacked with a mixed acid (3 mL HNO$_3$ + 2 mL HF + 1 mL H$_2$O$_2$). The accuracy of the PN-
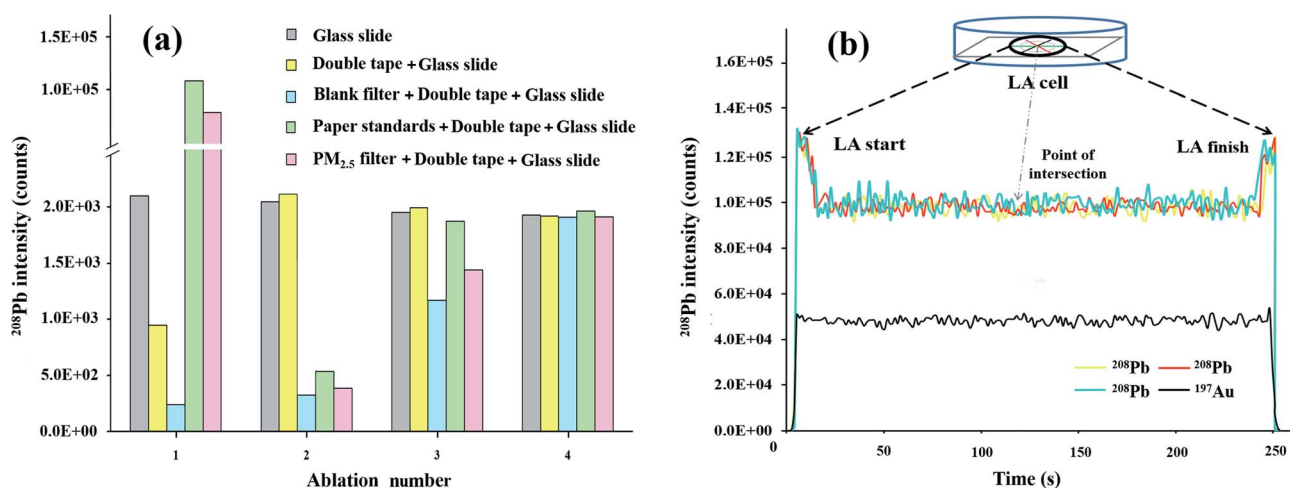

Fig. 3 LA–ICP–MS analysis to determine the element of Pb in different materials: (a) intensities of ^{208}Pb in five materials corresponding to the number of ablation sequences at the same location. (b) Signal profiles of ^{208}Pb obtained by LA–ICP–MS through three random lines scan across self-made filter paper (~8.0 mm); ^{197}Au is also shown.

Table 2 Analytical performance of the developed calibration method with the use of Au as IS in LA-ICP-MS ($n = 11$)

Elements	R^2		RSD%	LOD ($\mu g\ g^{-1}$)
	Without Au	With Au		
Mg	0.976	0.9984	8.4	0.06
K	—	—	6.3	0.33
Cr	0.983	0.9990	9.7	0.13
Mn	0.963	0.9986	8.3	0.06
Fe	0.956	0.9891	9.4	0.49
Ni	0.988	0.9989	6.5	0.07
Cu	0.981	0.9992	6.0	0.05
Zn	0.964	0.9989	6.8	0.08
As	0.993	0.9993	5.7	0.03
Sr	0.994	0.9991	4.3	0.01
Cd	0.996	0.9995	4.8	0.02
Ba	0.983	0.9986	5.7	0.02
Pb	0.992	0.9993	3.2	0.03

ICP-MS technique and the method recovery were evaluated by analyzing the certified reference materials NIST 1648a and 1573a.

Five self-made cellulose papers were used as calibration standards (Fil-0 to Fil-4) for the construction of calibration curves for each element of interest, with element concentrations ranging from 0 to 180 $\mu g\ g^{-1}$. LA-ICP-MS measurement was repeated six times on each self-made standard using scan lines with a length of 4.0 mm under the conditions specified in the Experimental section. Each line was ablated individually and in random positions over the paper disk. Table 2 summarizes the calibration results with and without the use of internal standardization ([197]Au as IS) for specific analytes to correct the differences in aerosol introduction, transmission, atomization, and ionization efficiency during measurement by LA-ICP-MS. It can be observed that the R^2 values of all elements (excerpt Fe) were higher than 0.998, and a better precision was obtained (RSD <10%) when IS was used (Fig. 4), indicating that Au is feasible for correcting the corresponding differences and confirming the good correlation between the effective concentrations of the paper standards and signal response of the ablated aerosol. The poor calibration curve of [54]Fe might be due to the occurrence of polyatomic interference. However, despite the poor linear calibration obtained for Fe, a suitable accuracy was
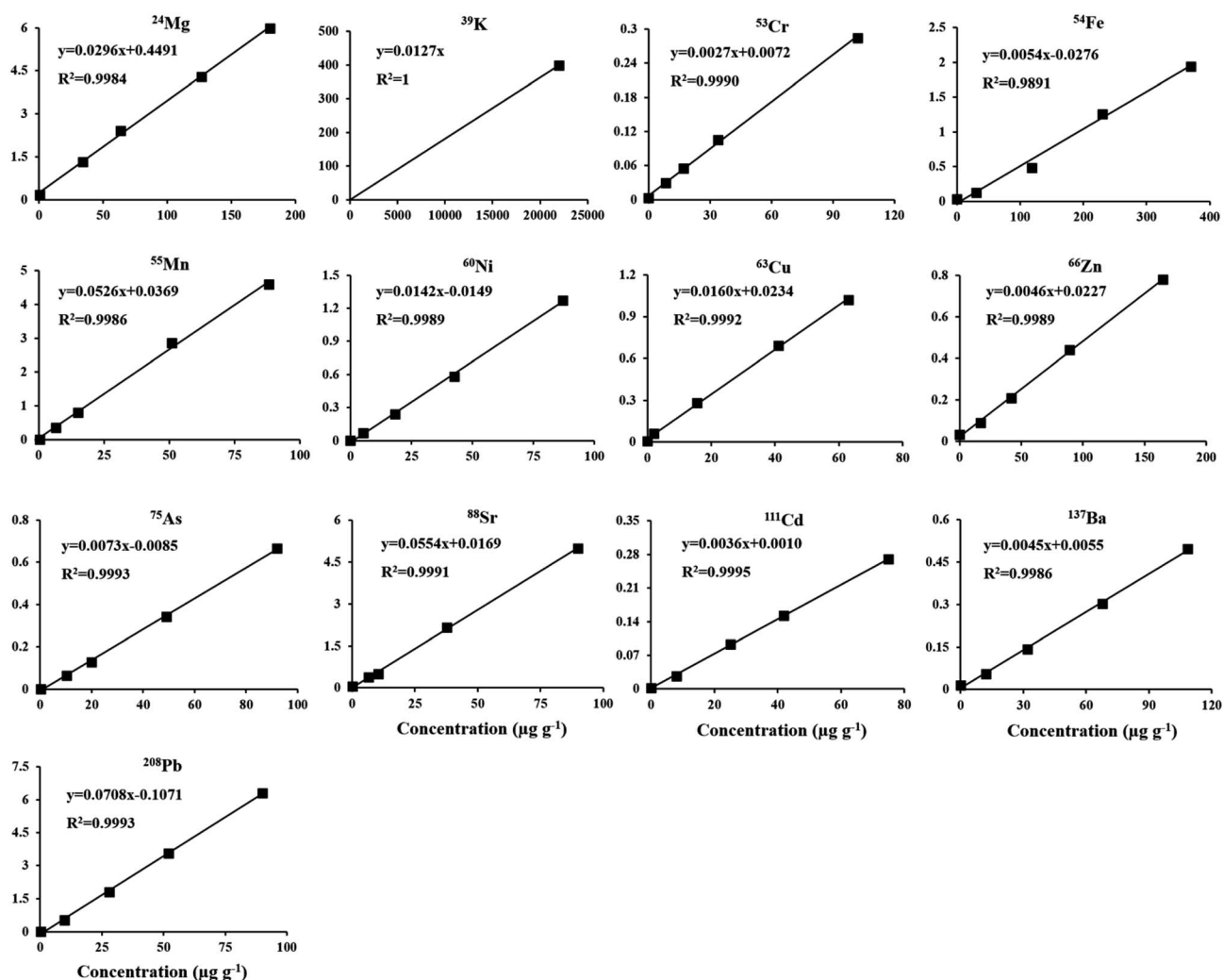

Fig. 4 Calibration curves of 13 elements in the solid filter paper standards measured by LA-ICP-MS with [197]Au as the internal standard.

Table 3 Results for the analysis of NIST 1648a and 1573a materials by PN-ICP-MS and LA-ICP-MS using our self-made papers as external standards ($n = 6$, $\mu g\ g^{-1}$)

	Urban dust (NIST 1648a)			Tomato leaves (NIST 1573a)		
Analyte	Certified	PN-ICP-MS	LA-ICP-MS	Certified	PN-ICP-MS	LA-ICP-MS
Mg	8130 ± 120	8255 ± 180	8673 ± 210	12 000	11 760 ± 420	12 640 ± 360
K	10 560 ± 490	11 210 ± 510	11 502 ± 470	26 760 ± 480	27 190 ± 510	28 630 ± 440
Cr	402 ± 13	418 ± 35	424 ± 24	1.99 ± 0.03	1.94 ± 0.04	2.10 ± 0.05
Mn	790 ± 44	789 ± 47	825 ± 35	246 ± 7.1	236 ± 4.9	261 ± 5.6
Fe	39 200 ± 2100	40 323 ± 2600	35 580 ± 2100	368 ± 4.3	375 ± 8.3	402 ± 9.2
Ni	81.1 ± 6.8	83.2 ± 5.5	86 ± 7.9	1.58 ± 0.04	1.56 ± 0.07	1.66 ± 0.11
Cu	610 ± 70	622 ± 54	580 ± 84	4.70 ± 0.14	4.57 ± 0.15	4.82 ± 0.20
Zn	4800 ± 270	4833 ± 320	5066 ± 350	30.9 ± 0.55	31.5 ± 0.93	33.5 ± 1.0
As	115.5 ± 3.9	120 ± 6.4	126 ± 7.1	0.11 ± 0.01	0.12 ± 0.01	0.15 ± 0.02
Sr	215 ± 17	223 ± 19	202 ± 21	85	86.3 ± 5.4	90.2 ± 6.8
Cd	73.7 ± 2.3	79.5 ± 4.7	80 ± 7.0	1.52 ± 0.03	1.53 ± 0.07	1.63 ± 0.05
Ba	698[a]	706 ± 43	757 ± 40	63	65.8 ± 4.5	66.8 ± 5.9
Pb	6550 ± 330	6611 ± 290	6785 ± 440	—[b]	0.53 ± 0.01	0.52 ± 0.03

[a] GeoReM.[39] [b] No available value.

Table 4 Results for the analysis of actual PM$_{2.5}$ atmospheric samples by LA-ICP-MS and the conventional liquid method ($n = 60$; expressed as content in gas, ng m^{-3}, average ± SD)

	BG							
	Spring		Summer		Autumn		Winter	
Element	Solution	LA	Solution	LA	Solution	LA	Solution	LA
Mg	814 ± 78	788 ± 50	403 ± 53	380 ± 39	686 ± 107	647 ± 80	1866 ± 160	1720 ± 155
K	2103 ± 180	2210 ± 230	509 ± 72	530 ± 81	1005 ± 118	970 ± 60	3121 ± 240	3250 ± 200
Cr	15 ± 2.2	17 ± 1.3	7.6 ± 1.1	8.1 ± 1.0	23 ± 2.6	25 ± 1.3	37 ± 3.8	38 ± 4.0
Fe	1756 ± 220	1570 ± 170	872 ± 118	866 ± 78	1304 ± 170	1195 ± 130	2511 ± 310	2417 ± 270
Mn	27 ± 3.6	30 ± 3.8	46 ± 5.7	50 ± 5.2	62 ± 7.4	69 ± 7.7	95 ± 12	103 ± 11
Ni	15 ± 2.1	16 ± 1.8	3.5 ± 0.6	3.9 ± 0.5	13 ± 2.0	14 ± 1.3	31 ± 2.6	35 ± 3.1
Cu	31 ± 3.5	34 ± 2.9	6.3 ± 0.9	7.0 ± 1.1	23 ± 4.1	21 ± 3.3	40 ± 4.6	36 ± 4.3
Zn	203 ± 33	224 ± 28	128 ± 22	140 ± 27	189 ± 20	203 ± 21	295 ± 32	297 ± 25
As	32 ± 3.0	34 ± 2.4	8.2 ± 1.3	9.0 ± 0.7	16 ± 1.4	18 ± 1.3	24 ± 3.1	27 ± 3.0
Ba	29 ± 3.4	31 ± 2.4	14 ± 1.8	12 ± 1.5	27 ± 2.2	27 ± 1.6	33 ± 2.0	37 ± 2.2
Sr	13 ± 2.0	15 ± 1.7	2.9 ± 0.4	3.1 ± 0.6	8.8 ± 1.1	9.6 ± 1.3	19 ± 2.3	21 ± 2.1
Cd	3.2 ± 0.5	3.5 ± 0.4	2.7 ± 0.3	2.4 ± 0.3	3.5 ± 0.4	3.3 ± 0.4	5.8 ± 0.7	6.3 ± 0.7
Pb	117 ± 15	124 ± 11	50 ± 5.2	45 ± 3.8	122 ± 21	118 ± 10	136 ± 14	146 ± 12

	LN							
	Spring		Summer		Autumn		Winter	
Elements	Solution	LA	Solution	LA	Solution	LA	Solution	LA
Mg	704 ± 76	727 ± 80	234 ± 29	240 ± 27	520 ± 49	540 ± 34	1183 ± 120	1130 ± 120
K	1077 ± 130	940 ± 90	441 ± 58	403 ± 45	852 ± 110	910 ± 95	1840 ± 190	2030 ± 200
Cr	6.5 ± 0.7	7.2 ± 0.8	1.2 ± 0.2	1.3 ± 0.1	4.0 ± 0.5	3.8 ± 0.3	8.4 ± 0.5	8.7 ± 0.9
Fe	1407 ± 170	1433 ± 160	688 ± 92	758 ± 94	1113 ± 140	1168 ± 120	2022 ± 230	2018 ± 190
Mn	62 ± 7.8	66 ± 7.2	34 ± 3.5	38 ± 3.6	44 ± 4.0	48 ± 3.9	79 ± 8.7	86 ± 6.8
Ni	15 ± 2.2	13 ± 1.4	9.9 ± 1.1	11 ± 0.7	12 ± 1.2	11 ± 0.6	27 ± 0.3	24 ± 0.3
Cu	23 ± 2.8	26 ± 1.9	9.6 ± 0.9	10 ± 0.9	17 ± 2.3	15 ± 1.2	34 ± 2.0	33 ± 2.2
Zn	82 ± 10	80 ± 8.2	41 ± 2.3	42 ± 2.6	53 ± 8.9	58 ± 4.1	115 ± 13	110 ± 10
As	9.9 ± 1.1	11 ± 1.0	3.1 ± 0.5	2.9 ± 0.3	7.8 ± 4.2	7.6 ± 0.9	16 ± 1.8	16 ± 1.3
Ba	14 ± 2.1	15 ± 1.5	3.7 ± 1.2	3.4 ± 0.9	9.4 ± 1.1	9.8 ± 0.7	22 ± 2.4	23 ± 1.6
Sr	7.5 ± 0.9	7.5 ± 0.6	4.1 ± 0.5	4.5 ± 0.3	5.6 ± 0.3	5.9 ± 0.4	4.1 ± 0.5	4.3 ± 0.5
Cd	1.6 ± 0.2	1.4 ± 0.2	0.34 ± 0.15	0.32 ± 0.09	0.78 ± 0.06	0.79 ± 0.05	2.2 ± 0.3	2.4 ± 0.3
Pb	64 ± 4.7	68 ± 3.2	21 ± 3.7	23 ± 1.6	52 ± 5.9	56 ± 5.2	83 ± 8.8	87 ± 6.0

obtained when this calibration curve was used for quantitative elements in the samples. The high-concentration inorganic element (*i.e.*, K) was calibrated using a single point equivalent to those in the $PM_{2.5}$ samples. Limits of detection established for LA-ICP-MS were obtained *via* the ablation of 11 lines on the procedural blank filter paper containing 0.5% HNO_3, with values ranging from 0.01 (Sr) to 0.49 μg g^{-1} (Fe).

The accuracy of the method was evaluated by analyzing two CRMs (Table 3). The relative errors between the measured and certified concentrations could be calculated using "RE = $(C_m - C_t)/C_t \times 100\%$", where "$C_m$" represents the measured concentrations determined by PN/LA-ICP-MS, and "C_t" represents the certified concentrations. As shown in Table 3, although the ashless cellulose filter paper did not completely match the CRM material matrix, most of the measured concentrations in CRMs *via* LA-ICP-MS using cellulose paper as the calibration standard were consistent with the certified values (average relative errors, RE < 10%).

3.2.4. $PM_{2.5}$ HEC analysis using LA-ICP-MS. To evaluate the applicability of our method for actual airborne matter, multi-element concentrations in $PM_{2.5}$ from suburban and downtown Hangzhou, China were analyzed. The average of the values from 60 samples was used as the final element concentration at each sampling point for each season (removing the extreme and abnormal values). In addition, the reference values of elements in $PM_{2.5}$ at BG and LN were determined *via* conventional liquid analysis and divided by the volume of the sample air. As shown in Table 4, satisfactory results were obtained *via* the LA-ICP-MS method, and the determined values were in good agreement with the reference concentrations. In conclusion, it was demonstrated that the calibration strategy developed in this study, which combines filter paper standards as external standards and a thin layer of gold as a pseudo IS, could be used for the quantitative determination of HEC in $PM_{2.5}$ samples.

In Table 4, it can be observed that in $PM_{2.5}$, ten trace elements (Cr, Mn, Ni, Cu, Zn, As, Sr, Cd, Ba, and Pb) played a very small part in the overall detected elements at BG (11.3%) and LN (7.9%), respectively. However, Mg, K, and Fe, which belong to the crustal elements, were dominant, accounting for 88.7% and 92.1%, respectively. In winter, the concentrations of the elements reached the highest values at the two sampling points, which might be attributed to the local sources of pollutants (*e.g.*, vehicle exhaust, coal consumption, and industrial activity) and less rain. In contrast, the lowest element concentrations were determined in summer, possibly because the city is often influenced by rainfall, which is an effective method to remove atmospheric particles.

3.3. Sources of elements

In previous studies, the EF model was often used to trace the sources of elements and evaluate the influence of human factors on the concentration of particulate matter-related elements,[40,41] calculated using the following equation:

$$EF = \frac{\left(\dfrac{X_i}{X_{ref}}\right)_{aerosol}}{\left(\dfrac{X_i}{X_{ref}}\right)_{crust}}$$

where X_i (X_{ref}) is the analyzed (reference) element content in the aerosol or crust. In this study, the content of elements in the surface soil of China was taken as the element concentration in the crust, and iron was selected as the reference element to calculate the element EFs in $PM_{2.5}$ collected at BG and LN.[42-44] As shown in Fig. 5, the EFs for different elements from the two sampling points were similar; however, each element was unique and could be divided into three categories: EF ≦ 10 (*i.e.*, Mg, K, Cr, Mn, Fe, and Sr), demonstrating that these elements were mainly related to natural pollution; EF ≦ 100 (*i.e.*, Ni, Cu, As, and Ba), indicating that the spread of these elements might be mainly the result of human activities; and EF ≦ 1000 (*i.e.*, Zn, Cd, and Pb), showing that the spread of these elements was related to the industrial or automobile emissions in Hangzhou. Although this method could not accurately reflect the sources of elements in $PM_{2.5}$, its results provide an auxiliary tool for element pollution analysis and hazard assessment.
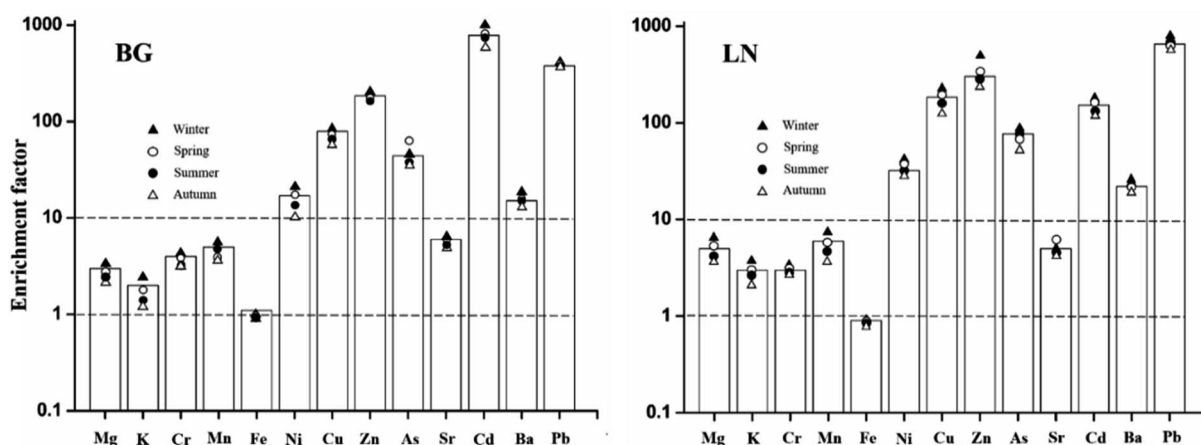

Fig. 5 Enrichment factors for elements in $PM_{2.5}$ at BG and LN.

4. Conclusions

A simple procedure for rapid quantification of HEC in PM$_{2.5}$ samples using LA-ICP-MS was developed. For LA-ICP-MS analysis, self-made external calibration standards were synthesized by immersing cellulose papers in standard solutions and covering them with a thin gold layer as a pseudo IS. The homogeneity of the analyte distribution was studied, and the results demonstrated that elements were homogeneously distributed in the ashless cellulose paper centers with slight fluctuations (RSDs $\leqq$ 8%), which meets the crucial requirement for an LA-ICP-MS reference material. The limits of detection established for LA-ICP-MS were obtained by the ablation of 11 lines on the procedural blank filter paper containing 0.5% HNO$_3$, with values ranging from 0.01 (Sr) to 0.49 μg g^{-1} (Fe). The proposed method was validated by analysis of NIST 1648a, NIST 1573a, and actual PM$_{2.5}$ samples with acceptable analytical errors (<13%) for most elements. In addition, the variations in mass concentrations and sources of PM$_{2.5}$ in Hangzhou were investigated using this method, and the main heavy elemental components of PM$_{2.5}$ showed drastic reductions in summer compared with those in other seasons. The present direct solid sampling method not only reduces the long sample preparation time and cumbersome process but can also be potentially expanded to study multi-element spatial distribution in airborne filter materials.

Author contributions

Conceptualization, Methodology, Original Draft Preparation, and Software: Lei Qiao. Investigation and Writing—Review & Editing: Ruijie Zhang. Formal Analysis and Visualization: Jing Qiao. Resources and Funding Acquisition: Zhiwei Wu. Validation, Writing—Review & Editing, Supervision, and Funding Acquisition: Xiaoyan He.

Conflicts of interest

The authors declare that they have no known competing financial interests or personal relationships that could have influenced the work reported in this paper.

Acknowledgements

References

1 Y. Lin, Y. Li, K. T. T. Amesho, S. Shangdiar, F. Chou and P. Cheng, *Sci. Total Environ.*, 2020, **739**, 139942–139951.

2 J. Yang, J. Jung, J. Ryu and J. J. Yoh, *Chemosphere*, 2020, **257**, 127237–127246.

3 D. G. Streets, J. S. Fu, C. J. Jang, J. Hao, K. He, X. Tang, Y. Zhang, Z. Wang, Z. Li, Q. Zhang, L. Wang, B. Wang and C. Yu, *Atmos. Environ.*, 2007, **41**, 480–492.

4 A. Przybysz, A. Saebo, H. M. Hanslin and S. W. Gawronski, *Sci. Total Environ.*, 2014, **481**, 360–369.

5 M. Park, H. S. Joo, K. Lee, M. Jang, S. D. Kim, I. Kim, L. J. S. Borlaza, H. Lim, H. Shin, K. Hyuckchung, Y. Choi, S. G. Park, M. Bae, J. Lee, H. Song and K. Park, *Sci. Rep.*, 2018, **8**, 1–11.

6 S. L. Ng, L. S. Chan, K. C. Lam and W. K. Chan, *Environ. Monit. Assess.*, 2003, **89**, 221–232.

7 H. Yang, J. Wang, M. Chen, D. Nie, F. Shen, Y. Lei, P. Ge, T. Gu, X. Gai, X. Huang and Q. Ma, *Chemosphere*, 2020, **254**, 126851–126859.

8 Y. Han, H. Kim, S. Cho, P. Kim and W. Kim, *Atmos. Res.*, 2015, **153**, 416–428.

9 F. K. Duan, K. B. He, Y. L. Ma, F. M. Yang, X. C. Yu, S. H. Cadle, T. Chan and P. A. Mulawa, *Sci. Total Environ.*, 2006, **355**, 264–275.

10 D. Sanchez-Rodas, A. M. Sanchez De La Campa and L. Alsioufi, *Anal. Chim. Acta*, 2015, **898**, 1–18.

11 P. Kulkarni, S. Chellam, J. B. Flanagan and R. K. M. Jayanty, *Anal. Chim. Acta*, 2007, **599**, 170–176.

12 X. Zheng, X. Xu, T. A. Yekeen, Y. Zhang, A. Chen, S. S. Kim, K. N. Dietrich, S. Ho, S. Lee, T. Reponen and X. Huo, *Aerosol Air Qual. Res.*, 2016, **16**, 388–397.

13 A. Ari, P. E. Ari and E. O. Gaga, *Talanta*, 2020, **208**, 120350–120358.

14 T. Okuda, J. Kato, J. Mori, M. Tenmoku, Y. Suda, S. Tanaka, K. B. He, Y. L. Ma, F. Yang, X. C. Yu, F. K. Duan and Y. Lei, *Sci. Total Environ.*, 2004, **330**, 145–158.

15 S. Gligorovski, J. T. Van Elteren and I. Grgic, *Sci. Total Environ.*, 2008, **407**, 594–602.

16 M. S. Robinson, I. Grgic, V. S. Selih, M. Sala, M. Bitsui and J. T. van Elteren, *Atmos. Meas. Tech.*, 2017, **10**, 1823–1830.

17 R. J. C. Brown, K. E. Jarvis, B. A. Disch, S. L. Goddard and A. S. Brown, *J. Environ. Monit.*, 2009, **11**, 2022–2029.

18 X. Tang, Y. Qian, Y. Guo, N. Wei, Y. Li, J. Yao, G. Wang, J. Ma and W. Liu, *Spectrochim. Acta, Part B*, 2017, **138**, 18–22.

19 R. J. C. Brown and M. J. T. Milton, *Chem. Soc. Rev.*, 2007, **36**, 904–913.

20 D. Clases, R. G. de Vega, P. A. Adlard and P. A. Doble, *J. Anal. At. Spectrom.*, 2019, **34**, 407–412.

21 L. Guo, Q. Li, Y. Chen, G. Zhang, Y. Xu and Z. Wang, *J. Anal. At. Spectrom.*, 2020, **35**, 1441–1449.

22 X. Liao, T. Luo, S. Zhang, W. Zhang, K. Zong, Y. Liu and Z. Hu, *J. Anal. At. Spectrom.*, 2020, **35**, 1071–1079.

23 Y. Hsieh, L. Chen, H. Hsieh, C. Huang and C. Wang, *J. Anal. At. Spectrom.*, 2011, **26**, 1502–1508.

24 G. D. S. Pessoa, C. A. Lopes Junior, K. C. Madrid and M. A. Z. Arruda, *Talanta*, 2017, **167**, 317–324.

25 M. Voss, M. A. G. Nunes, G. Corazza, E. M. M. Flores, E. I. Mueller and V. L. Dressler, *Talanta*, 2017, **170**, 488–495.

26 Y. Ke, J. Zhou, X. Yi, Y. Sun, J. Shao, S. You, W. Wang, Y. Tang and C. Tu, *J. Anal. At. Spectrom.*, 2020, **35**, 886–895.

27 J. Lear, D. J. Hare, F. Fryer, P. A. Adlard, D. I. Finkelstein and P. A. Doble, *Anal. Chem.*, 2012, **84**, 6707–6714.

28 M. Togao, S. M. M. Nakayama, Y. Ikenaka, H. Mizukawa, Y. Makino, A. Kubota, T. Matsukawa, K. Yokoyama, T. Hirata and M. Ishizuka, *Chemosphere*, 2020, **238**, 1–8.

29 A. Ugarte, N. Unceta, C. Pecheyran, M. A. Goicolea and R. J. Barrio, *J. Anal. At. Spectrom.*, 2011, **26**, 1421–1427.

30 C. F. Wang, M. C. Yuan, C. Y. Chang and S. C. Huang, *J. Radioanal. Nucl. Chem.*, 2006, **268**, 15–23.

31 C. Wanga, S. Jenga, C. C. Lina and P. Chiangb, *Anal. Chim. Acta*, 1998, **368**, 11–19.

32 M. A. G. Nunes, M. Voss, G. Corazza, E. M. M. Flores and V. L. Dressler, *Anal. Chim. Acta*, 2016, **905**, 51–57.

33 M. Bonta, B. Hegedus and A. Limbeck, *Anal. Chim. Acta*, 2016, **908**, 54–62.

34 M. Bonta, H. Lohninger, V. Laszlo, B. Hegedus and A. Limbeck, *J. Anal. At. Spectrom.*, 2014, **29**, 2159–2167.

35 Y. Ke, J. Zhou, L. Qiao, M. Zhang, W. Guo, L. Jin and S. Hu, *Anal. Methods*, 2019, **11**, 2129–2137.

36 G. Liu, F. Yuan, Y. Deng, F. Wang, N. C. White, J. M. Huizenga, Y. Li, X. Li and T. Zhou, *Ore Geol. Rev.*, 2020, **117**, 1–14.

37 Y. Liu, Z. Hu, S. Gao, D. Guenther, J. Xu, C. Gao and H. Chen, *Chem. Geol.*, 2008, **257**, 34–43.

38 V. X. Nguyen and K. J. Stebe, *Phys. Rev. Lett.*, 2002, **88**, 164501–164504.

39 K. P. Jochum, L. Nohl, K. Herwig, E. Lammel, B. Stoll and A. W. Hofmann, *Geostand. Geoanal. Res.*, 2005, **29**, 333–338.

40 L. H. Tecer, G. Tuncel, F. Karaca, O. Alagha, P. Suren, A. Zararsiz and R. Kirmaz, *Atmos. Res.*, 2012, **118**, 153–169.

41 C. A. Belis, F. Karagulian, B. R. Larsen and P. K. Hopke, *Atmos. Environ.*, 2013, **69**, 94–108.

42 W. H. Zoller, E. S. Gladney and R. A. Duce, *Science*, 1974, **183**, 198–200.

43 C. Reimann and P. D. Caritat, *Environ. Sci. Technol.*, 2000, **34**, 5084–5091.

44 H. Cheng, K. Li, M. Li, K. Yang, F. Liu and X. Cheng, *Earth Sci. Front.*, 2014, **21**, 265–306.